

Heterologous production of a new lasso peptide brevunsin in *Sphingomonas subterranea*

メタデータ	言語: eng 出版者: 公開日: 2020-06-02 キーワード (Ja): キーワード (En): 作成者: 逸見, 光, 中川, 博之 メールアドレス: 所属:
URL	https://repository.naro.go.jp/records/3438

This work is licensed under a Creative Commons Attribution-NonCommercial-ShareAlike 3.0 International License.



1 Heterologous production of a new lasso peptide brevunsin in *Sphingomonas*

2 *subterranea*

3 Running headline: Heterologous production of brevunsin

4 Authors: Shinya Kodani,^{1,2,3} Hikaru Hemmi,⁴ Yuto Miyake,² Issara Kaweewan,³ and

5 Hiroyuki Nakagawa^{4,5}

6 Affiliations: ¹College of Agriculture, Academic Institute, Shizuoka University,

7 Shizuoka 422-8529, Japan; ²Graduate School of Integrated Science and Technology,

8 Shizuoka University, Shizuoka 422-8529, Japan; ³Graduate School of Science and

9 Technology, Shizuoka University, Shizuoka 422-8529, Japan; ⁴Food Research Institute,

10 National Agriculture and Food Research Organization (NARO), Ibaraki 305-8642,

11 Japan; ⁵Advanced Analysis Center, National Agriculture and Food Research

12 Organization (NARO), Ibaraki 305-8642, Japan

13

14

15 *To whom correspondence should be addressed: Shinya Kodani, College of Agriculture,

16 Academic Institute, Shizuoka University, 836 Ohya, Suruga-ku, Shizuoka 422-8529

17 Japan, Tel/Fax; +81(54)238-5008, E-mail; kodani.shinya@shizuoka.ac.jp

18

19 **Abstract**

20 A shuttle vector pHSG396Sp was constructed to perform gene expression using
21 *Sphingomonas subterranea* as a host. A new lasso peptide biosynthetic gene cluster,
22 derived from *Brevundimonas diminuta*, was amplified by PCR and integrated to afford a
23 expression vector pHSG396Sp-12697L. The new lasso peptide brevunsin was
24 successfully produced by *S. subterranea*, harboring the expression vector, with a high
25 production yield (10.2 mg from 1 L culture). The chemical structure of brevunsin was
26 established by NMR and MS/MS experiments. Based on the information obtained from
27 the NOE experiment, the three-dimensional structure of brevunsin was determined,
28 which indicated that brevunsin possessed a typical lasso structure. This expression
29 vector system provides a new heterologous production method for unexplored lasso
30 peptides that are encoded by bacterial genomes.

31

32

33 **Introduction**

34 A lasso peptide is a unique peptide, normally 15-25 amino acids in length, which
35 possesses the common motif of a knot structure in the molecule. Based on its biosynthetic
36 system, it is classified with the ribosomally biosynthesized and post-translationally
37 modified peptides (RiPPs) [3, 26, 28, 36]. In the biosynthesis of the lasso peptide, an
38 isopeptide bond is formed between the amino group of the N-terminal amino acid and the
39 β - or γ -carboxyl group of Asp or Glu at the 7th - 9th position from the N-terminus, which
40 results in a macrolactam ring [27, 31, 33]. The tail of the C-terminal linear peptide
41 normally passes through the ring, which is defined as the “lasso” structure. The first lasso
42 peptide, named microcin J25, was isolated from a culture of *Escherichia coli* [35]. The
43 biosynthetic gene cluster for microcin J25 (about 4.8 kbp) was reported to include four
44 genes: a precursor peptide coding gene (gene A: McjA), two maturation enzyme coding
45 genes (gene B: McjB and gene C: McjC), and an ATP-binding cassette transporter gene
46 (gene D: McjD) [37]. Normally, the lasso peptide biosynthetic genes in proteobacteria
47 have the same set of the genes, although the transporter gene is optional.

48 Recently the genome mining method has become a powerful tool to find new lasso
49 peptides, due to the accumulation of bacterial genome data [29, 20, 13, 32]. The
50 prediction system for RiPPs, named RODEO (Rapid ORF Description and Evaluation

51 Online), was developed, resulting in the discovery of six new lasso peptides [38]. The
52 genome-mining approach and heterologous production using *Escherichia coli* as host
53 cells have been performed to produce new lasso peptides [15, 14, 13, 12, 11, 10, 41]. To
54 produce useful functional molecule by modifying natural lasso peptide, several attempts
55 were reported. Recently, RGD peptide motif was integrated into the lasso peptide
56 microcin J25 to yield recombinant microcin J25 which had a highly potent and selective
57 $\alpha\beta3$ integrin inhibitory activity [10]. The lasso peptide benenodin-1 was reported to
58 exhibit conformational switching between two distinct threaded conformers upon
59 actuation by heat, like a rotaxane switch [39]. In any case, the heterologous *E. coli*
60 expression system is problematic in that the amount of the lasso peptide produced is not
61 very high without engineering the DNA sequence of the gene cluster [40]. To exploit
62 lasso peptide gene clusters, improved method to perform heterologous production
63 system is needed to obtain larger amount of new lasso peptide. We recently found
64 production of a new lasso peptide, named subterisin, in a culture of *Sphingomonas*
65 *subterranea* with high yield (15.0 mg from 1 L culture) [24]. On the other hand,
66 Hayashi and Kurusu reported the construction of stable shuttle vectors between *E. coli*
67 and *Sphingomonas* species [8, 9]. The GC content of genome of *S. subterranea* is high
68 (approximately 63 %) compared to that of *Escherichia coli* (approximately 50 %), so

69 there is an advantage to use *S. subterranea* as a host for expression of gene with high
70 GC content. We proposed that expression of the lasso peptide biosynthetic genes with
71 high GC content in *S. subterranea* could result in a large amount of production of the
72 exogenous lasso peptide. Based on this speculation, we accomplished the construction
73 of a shuttle vector between *E. coli* - *Sphingomonas* sp. and heterologous production of a
74 new lasso peptide named brevunsin in *S. subterranea*. Here, we describe the
75 heterologous production and structure determination of the new lasso peptide brevunsin.

76 **Materials and methods**

77 **Bacterial strains.**

78 The microorganisms (Bacterial strains including *Sphingomonas subterrenea* NBRC
79 16086^T, *Sphingobium yanoikuyae* NBRC 15102^T, *Brevundimonas diminuta* NBRC
80 12697^T, *Escherichia coli* NBRC 102203^T, *Pseudomonas aeruginosa* NBRC 12689^T,
81 *Bacillus subtilis* NBRC 13719^T, *Staphylococcus aureus* NBRC 100910^T, *Micrococcus*
82 *luteus* NBRC 3333^T; Yeast strains including *Saccharomyces cerevisiae* NBRC 2376,
83 *Schizosaccharomyces pombe* NBRC 0340; fungi strains including *Aspergillus niger*
84 NBRC 33023^T, *Aspergillus oryzae* NBRC 4290 were obtained from the NBRC culture
85 collection (NITE Biological Resource Center, Japan).

86 **Construction of the shuttle vector pHSG396Sp**

87 For the template for PCR amplification, the plasmid pYAN1 was purified from the cells
88 of *Sphingobium yanoikuyae* using an isolation kit (FastGene Plasmid Mini Kit,
89 NIPPON Genetics Co. Ltd, Tokyo, Japan). To construct the shuttle vector pHSG396Sp,
90 the sequence (1228 bp, including repA: WP_004213409.1) was amplified by PCR with
91 the template (pYAN1) and the primer pair YAN1-F1 and YAN1-R2 (Table S1), using a
92 high-fidelity Phusion polymerase (NEB, Frankfurt/Main, Germany), following the
93 manufacturer's instructions. The DNA fragment insert, including repA, and the
94 pHSG396 vector (Takara Bio Inc., Shiga, Japan) were double digested with HindIII
95 (NEB) and SalI (NEB), according to the manufacturer's instructions. The DNA
96 products were ligated using T4 DNA ligation mix (Takara Bio Inc.) to afford the shuttle
97 vector pHSG396Sp. *E. coli* DH5 α cells were transformed with 5 μ L of the ligation
98 mixture by chemical competence transformation, and the cells were plated on LB agar
99 medium (5 g tryptone, 2.5 g yeast extract, 5 g NaCl, and 15 g agar in 1 L distilled water)
100 containing chloramphenicol (final concentration: 20 μ g/mL). The plasmid pHSG396Sp
101 was purified using an isolation kit (FastGene Plasmid Mini Kit).

102 **Construction of the expression vector pHSG396Sp-12697L**

103 For the template for PCR amplification, genomic DNA was extracted from the cells of
104 *Brevundimonas diminuta* using DNeasy Blood & Tissue (Qiagen, Venlo, Netherlands).

105 The DNA fragment, including the lasso peptide brevunsin biosynthetic gene cluster
106 (2754 bp, *breA*, *breB*, and *breC*), was amplified by PCR with the template and the
107 primer pair of 12697L-F and 12697L-R (Table S1), using a high-fidelity Phusion
108 polymerase (NEB), following the manufacturer's instructions. The DNA fragment
109 insert, including the brevunsin biosynthetic gene cluster, and the shuttle vector
110 pHSG396Sp were digested with XbaI (NEB) and KpnI (NEB), according to the
111 manufacturer's instructions. The DNA products were ligated using T4 DNA ligation
112 mix (Takara Bio Inc.) to afford the vector pHSG396Sp-12697L. *E. coli* DH5 α cells
113 were transformed with 5 μ L of the ligation mixture by chemical competence
114 transformation, and the cells were plated on LB agar plates containing chloramphenicol
115 (final concentration: 20 μ g/mL). The plasmid pHSG396Sp-12697L was purified using
116 an isolation kit (FastGene Plasmid Mini Kit). The DNA sequences of the plasmids
117 (pHSG396Sp and pHSG396Sp-12697L) were determined by direct DNA sequencing
118 using Applied Biosystems 3730xl (Thermo Fisher Scientific, Inc., Massachusetts,
119 USA), as shown in Fig. S1 and S2.

120 **Transformation of the expression vector to *Sphingobium subterranea***

121 The plasmid pHSG396Sp or pHSG396Sp-12697L was transformed into *Sphingomonas*
122 *subterranea* using electroporation. The bacterium *S. subterranea* was cultured in 10 mL

123 of NBRC medium (number 802 liquid medium; 10 g peptone, 2 g yeast extract, and 1 g
124 $\text{MgSO}_4 \cdot 7\text{H}_2\text{O}$ in 1 L distilled water, pH 7.0) at 30 °C for 24 h with shaking at 50 rpm.
125 The cells were cooled on ice for 30 min, followed by centrifugation (4000 rpm, 4 °C, 10
126 min). The harvested cells were suspended in 10 ml of a cold 10% glycerol solution.
127 After centrifugation (4000 rpm, 4 °C, 10 min), the cells were harvested and resuspended
128 in 10 ml of a cold 10% glycerol solution. After centrifugation (4000 rpm, 4 °C, 10 min),
129 the harvested cells were resuspended in 0.1 mL of a cold 10% glycerol solution for
130 electroporation. The electroporation experiment for a 0.1 mL suspension of cells was
131 performed with the program “Ec3” (Voltage: 3.0 kV, 1 pulse) using a MicroPulser (Bio-
132 Rad Laboratories, California, USA). After electroporation, 0.5 mL of Super Optimal
133 Broth with Catabolic repressor (SOC) medium was immediately added to the cell
134 suspension. For the recovery of damage, the cells were incubated at 30 °C for 2 h. Then,
135 the *S. subterranea* cells were spread onto NBRC medium (number 802 agar medium; 10
136 g peptone, 2 g yeast extract, 1 g $\text{MgSO}_4 \cdot 7\text{H}_2\text{O}$, and 15 g agar in 1 L distilled water, pH
137 7.0) containing chloramphenicol (final concentration: 10 µg/mL). After incubation at
138 30 °C for 6 days, colonies were picked and checked by the colony PCR method to
139 obtain *S. subterranea* harboring pHSG396Sp or pHSG396Sp-12697L.

140 **Isolation of brevunsin**

141 *Sphingomonas subterranea* harboring pHSG396Sp-12697L was cultured using 1 L of
142 modified basal medium [16] containing chloramphenicol (20 µg/mL, final concentration)
143 with shaking of 120 rpm at 30 °C for 9 days. The modified basal medium was prepared
144 by adding the inorganic compounds (K₂SO₄, 2 g; K₂HPO₄, 3 g; NaCl, 1 g; NH₄Cl, 5 g;
145 MgSO₄•7H₂O, 80 mg; CuCl₂, 5 mg; MnSO₄•H₂O, 2.5 mg; FeCl₃•6H₂O, 5 mg;
146 CaCl₂•2H₂O, 5 mg) in 1L of distilled water with adjusting pH 7.0. After autoclaving,
147 the medium was supplemented with separately sterilized glucose and yeast extract at final
148 concentrations of 0.25%, 0.005%, respectively. The culture including bacterial cells
149 was evaporated using rotary evaporator to aqueous residue (about 20 mL). The aqueous
150 residue was extracted with MeOH (300 mL). After filtration with paper filter (Wattman
151 No. 1 filter, GE Healthcare Life Sciences, Illinois, USA), the MeOH extract was
152 concentrated to aqueous residue using rotary evaporator. The aqueous residue was
153 subjected to open column chromatography using hydrophobic resin CHP-20P (Mitsubishi
154 Chemical Co., Tokyo, Japan), eluted with 10% MeOH, 60% MeOH, and 100% MeOH.
155 The 60% MeOH fraction was subjected to HPLC analysis using ODS column (4.6 × 250
156 mm, 5 µm, Wakopak Handy-ODS, Wako Pure Chemical Industries Ltd., Osaka, Japan)
157 with gradient elution from 20% to 50% MeCN containing 0.05% trifluoroacetic acid for
158 20 min with UV detector set at 220 nm to detect brevunsin (retention time, 12.1 min, Fig.

159 S3) along with subterisin (retention time, 13.4 min, Fig. S3). For isolation of brevunsin,
160 the 60% MeOH fraction was repeatedly subjected to HPLC purification using ODS
161 column (4.6 × 250 mm, 5 μm, Wakopak Handy-ODS, Wako Pure Chemical Industries,
162 Ltd., Osaka, Japan) with isocratic elution at 22% MeCN containing 0.05% trifluoroacetic
163 acid with UV detector set at 220 nm to isolate 10.2 mg of brevunsin (retention time, 26.8
164 min, Fig. S4). The yield of brevunsin was weighed by precision balance (AW320,
165 SHIMADZU Co., Tokyo, Japan).

166 **Treatment of cyanogen bromide**

167 Brevunsin (0.5 mg) was dissolved in 1 ml of 70% HCOOH and treated for 4h at room
168 temperature with 0.1M cyanogen bromide. After cleavage, the reaction mixture was
169 centrifuged at 14500 rpm and the supernatant was concentrated by rotary evaporator and
170 completely lyophilized by freeze dryer. The residue was re-dissolved in 0.5 mL of
171 methanol and subjected to reversed-phase HPLC purification using ODS column (4.6 ×
172 250 mm, 5 μm, Wakopak Handy-ODS, Wako Pure Chemical Industries Ltd.) with
173 gradient elution from 20% to 70% MeCN containing 0.05% trifluoroacetic acid for 20
174 min with UV detector set at 220 nm to yield cleaved brevunsin.

175 **Mass spectrometry experiments**

176 Brevunsin or cleaved brevunsin was dissolved in 30% MeCN. The accurate mass
177 measurement was conducted using a Fourier-transform ion cyclotron resonance (FT-
178 ICR) mass spectrometer (ApexII 70e, Bruker Daltonics). Brevunsin sample was
179 appropriately diluted with 50% MeOH containing 0.1% formic acid was, and supplied
180 to FT-ICR mass spectrometer by direct infusion with electrospray ionization (ESI) in the
181 positive polarity. MALDI-TOF MS and MS/MS analysis was conducted using a
182 MALDI-TOF/TOF mass spectrometer (4800 *Plus* TOF/TOF analyzer, Sciex, CA,
183 USA). Brevunsin sample was mixed with equal volume of α -Cyano-4-
184 hydroxycinnamic acid (4-CHCA) (Shimadzu GLC Ltd., Tokyo) matrix solution
185 (prepared as 10 mg/mL in 50%AcCN containing 0.1% tri-fluoro acetic acid) in 1:1 ratio,
186 and aliquot of the mixture (0.5 μ L) was spotted onto a standard stainless plate. After
187 dried up, MS and MS/MS spectra were measured in the positive-ion mode with an
188 acceleration voltage of 20 kV. The mass spectrometer was tuned and calibrated using
189 calibration standards of YOKUDELNA (JEOL, Tokyo, Japan) and the peptide mixture
190 (Peptide Calibration Standard II, Bruker Daltonics), respectively, prior to the
191 measurements.

192 **NMR experiments**

193 A NMR sample was prepared by dissolving the purified peptide in 500 μ l of dimethyl
194 sulfoxide- d_6 (DMSO- d_6). All NMR spectra were obtained on Bruker Avance 600 and
195 Avance III HD 800 spectrometers with quadrature detection in the phase-sensitive mode
196 by States-TPPI (time proportional phase incrementation) and in the echo-antiecho
197 mode. One-dimensional (1D) ^1H , ^{13}C , DEPT-135 spectra were recorded at 25 $^\circ\text{C}$ with
198 15 ppm for proton and 239 ppm or 222 ppm for carbon. The following spectra were
199 recorded at 20, 25, or 30 $^\circ\text{C}$, respectively, with 15 ppm spectral widths in t_1 and t_2
200 dimensions: two-dimensional (2D) double quantum filtered correlated spectroscopy
201 (DQF-COSY), recorded with 512 and 1024 complex points in t_1 and t_2 dimensions; 2D
202 homonuclear total correlated spectroscopy (TOCSY) with DIPSI2 mixing sequence,
203 recorded with mixing time of 80 ms, 512 and 1024 complex points in t_1 and t_2
204 dimensions; 2D nuclear Overhauser effect spectroscopy (NOESY), recorded with
205 mixing times of 200 and 400 ms, 512 and 1024 complex points in t_1 and t_2 dimensions.
206 2D ^1H - ^{13}C heteronuclear single quantum correlation (HSQC) and heteronuclear multiple
207 bond connectivity (HMBC) spectra were acquired at 25 $^\circ\text{C}$ in the echo-antiecho mode.
208 The ^1H - ^{13}C HSQC and HMBC spectra were recorded with 1024×512 complex points
209 for 15 ppm in the ^1H dimension and 160 ppm or 222 ppm in the ^{13}C dimension,
210 respectively, at a natural isotope abundance. 2D ^1H - ^{15}N HSQC spectrum was recorded

211 with 1024×128 complex points for 15 ppm in the ^1H dimension and 40 ppm in the ^{15}N
212 dimension at a natural isotope abundance. All NMR spectra were processed using
213 TOPSPIN 3.5 (Bruker). Peak-picking and assignment were performed with Sparky
214 program (UCSF, <http://www.cgl.ucsf.edu/Research/Sparky.html>). Before Fourier
215 transformation, the shifted sinebell window function was applied to $t1$ and $t2$
216 dimensions. All ^1H and ^{13}C dimensions were referenced to $\text{DMSO-}d_6$ at 25 °C.

217 **Structure calculations**

218 Distance restraints were constructed from intensities of NOE cross peaks in 2D NOESY
219 spectra with mixing times of 200 ms, which were classified into four distance categories
220 (2.9, 3.5, 5.0, and 6.0 Å). Pseudo-atom corrections were made for non-stereospecifically
221 assigned methylene and methyl resonance [39]. An additional 0.5 Å were added to the
222 upper bounds for methyl protons [4]. Backbone Φ dihedral angle restraints were
223 evaluated from $^3J_{\text{HN}\alpha}$ values obtained from the high digital resolution 2D DQF-COSY
224 spectrum and intraresidue and sequential NOEs. Backbone ϕ -angles were restrained to $-$
225 $120^\circ \pm 40^\circ$ for $^3J_{\text{HN-H}\alpha} = 8.5 - 9$ Hz and $-120^\circ \pm 30^\circ$ for $^3J_{\text{HN-H}\alpha} > 9$ Hz. The additional
226 Φ dihedral angle restraint of $100^\circ \pm 80^\circ$ was applied to residues for which the
227 intraresidue HN-H α NOE was clearly weaker than the NOE between HN and the H α of
228 the preceding residue [5]. The solution structure of brevunsin was calculated by

229 simulated annealing protocol using distant and dihedral angle restraints with the
230 program CNS version 1.1 [2]. The Asp1-Glu9 isopeptide linkage was generated using a
231 manual patch of the “protein-allhdg.top” CNS file modified from the manual patch of
232 the “protein1.0.top” XPLOR-NIH file [34]. Three hundred structures were calculated, of
233 which the 15 structures of lowest energy were selected for structural analysis. The final
234 15 lowest-energy ensemble structures were analyzed by MOLMOL [23] and
235 PROCHECK-NMR [25], and graphics were created by MOLMOL. The atomic
236 coordinate data was deposited in the Protein Data Bank (PDB ID: 5ZCN).

237 **Thermostability test of brevunsin**

238 Concentration of brevunsin was adjusted to 0.5 mg/mL in DMSO. Aliquot sample (100
239 μ l each) was heated at 50 °C, 65°C, 80 °C, and 95 °C for 1 hr, followed by immediate
240 cooling to 4 °C. Each sample (50 μ l) was subjected to HPLC analysis using ODS column
241 (4.6 \times 250 mm, 5 μ m, Wakopak Handy-ODS, Wako Pure Chemical Industries Ltd., Osaka,
242 Japan) with gradient elution from 20% to 60% MeCN containing 0.05% trifluoroacetic
243 acid for 20 min with UV detector set at 220 nm.

244 **Modified Marfey’s method**

245 Brevunsin (1.0 mg) was subjected to acid hydrolysis with 6N HCl containing 3% phenol

246 and 1% mercaptoethanol at 110 °C for 16 h for detection of amino acids. The hydrolysates
247 were completely evaporated using rotary evaporator, followed by adding 200 µL of water.
248 10 µL of *N*α-(5-fluoro-2,4-dinitrophenyl)-L-leucinamide (L-FDLA, Tokyo Chemical
249 Industry Co., Ltd, Tokyo, Japan) in acetone (10 µg/µL) and 100 µL of 1M NaHCO₃
250 solution were added to the hydrolysate and the mixture was incubated at 80 °C for 3 min.
251 The reaction mixture was cooled down to room temperature before being neutralized with
252 50 µL of 2N HCl and diluted with 1 mL of 50% MeCN. For standard amino acid, each
253 amino acid was derivatized with L-FDLA and D-FDLA in the same method.
254 Approximately 30 µL of each FDLA derivatives was subjected to HPLC analysis with
255 C18 column (4.6 × 250 mm, Wakopak Handy ODS, WAKO Pure Chemical Industries
256 Ltd.). The DAD detector (MD-2018, JASCO, Tokyo, Japan) was used for detection of the
257 amino acid derivatives accumulating the data of the absorbance from 220nm to 420 nm.
258 The HPLC analysis was performed at a flow rate of 1 mL/min using solvent A (distilled
259 water containing 0.05% TFA) and solvent B (MeCN containing 0.05%TFA) with a linear
260 gradient mode from 0 min to 70 min, increasing percentage of solvent B from 25% to
261 60%. The retention times (min) of L- or D-FDLA derivatized amino acids in this HPLC
262 condition were following; L-Arg-D-FDLA (17.23 min), L-Arg-L-FDLA (22.24 min), L-
263 Asp-L-FDLA (23.43 min), L-Tyr-D-FDLA (24.09 min), L-Ser-L-FDLA (24.16 min), L-

264 Ser-D-FDLA (25.19min), L-Asp-D-FDLA (26.86 min), L-Glu-L-FDLA (28.12 min), L-
265 Glu-D-FDLA (30.43 min), L-Pro-L-FDLA (30.8 min), L-Ala-L-FDLA (32.69 min), L-
266 Tyr-L-FDLA (34.70 min), L-Pro-D-FDLA (35.89 min), L-Met-L-FDLA (38.53 min), L-
267 Ala-D-FDLA (39.77 min), L-allo-Ile-L-FDLA (43.43 min), L-Ile-L-FDLA (43.72 min),
268 L-Leu-L-FDLA (44.74 min), L-Phe-L-FDLA (46.22 min), L-allo-Ile-D-FDLA (49.27
269 min), L-Met-D-FDLA (49.33 min), L-Ile-D-FDLA (49.35 min), L-Val-D-FDLA (51.77
270 min), L-Phe-D-FDLA (54.16 min), L-Leu-D-FDLA (59.17 min), and L-Val-L-
271 FDLA(59.67 min).

272 **Antimicrobial assays**

273 The testing microorganisms were following: *E. coli*, *P. aeruginosa*, *B. subtilis*, *S. aureus*,
274 *M. luteus*, *S. cerevisiae*, *S. pombe*, *A.niger*, and *A. oryzae*. The testing microorganisms
275 were cultivated using nutrient agar medium (peptone 5 g, beef extract 3 g, NaCl 5g, agar
276 15 g in 1 L of distilled water, pH 7.3) for *E. coli*, *P. aeruginosa*, *B. subtilis*, *S. aureus*, *M.*
277 *luteus*, *S. cerevisiae* or ISP2 agar medium (malt extract 10 g, yeast extract 4 g, glucose 4
278 g, agar 15 g in 1 L of distilled water, pH 7.3) for *S. cerevisiae*, *S. pombe*, *A.niger*, *A.*
279 *oryzae* with incubation at 30°C. The peptide was dissolved in DMSO at the concentration
280 of 10 mg/mL. After the testing microorganisms were inoculated on the surface of agar
281 medium, the paper disk with 50 µg of the peptide (5 µL) or negative control (DMSO, 5

282 μL) was placed onto the agar plate. After incubation for 2 days at 30 °C, the formation
283 of inhibition zone around the well was used for evaluation of antimicrobial activity.

284 **Results and Discussion**

285 Previously, Hegemann *et al.* indicated the distribution of the lasso peptide biosynthetic
286 gene cluster in proteobacteria [14, 30]. In the reports [14, 30], an interesting lasso
287 peptide biosynthetic gene cluster was found among the genome data for *Brevundimonas*
288 *diminuta* (Fig. 1). The biosynthetic gene cluster had a typical set of lasso peptide
289 biosynthetic genes, including the genes *breA* (accession number: EGF94505.1), *breB*
290 (EGF94506.1), and *breC* (EGF94507.1). The leader peptide sequence in the lasso
291 peptide precursor normally has the conserved sequence -Thr-X- before the core peptide
292 sequence, and the first amino acid of the core peptide is often Gly, Ser, or Cys in most
293 cases. However, the core peptide sequence of brevunsin started with Asp (Fig. 1), and
294 this was unusual for a lasso peptide core peptide. It was of great interest to clarify
295 whether this biosynthetic gene cluster functioned to afford the expected lasso peptide
296 brevunsin. Firstly we performed detection of lasso peptide production in extract of
297 culture of *B. diminuta* by HPLC and ESI-MS, following the previous report [24]. As a
298 result, production of the expected lasso peptide brevunsin was not observed (Data not
299 shown). Therefore, we planned to perform heterologous production of the lasso peptide

300 named brevunsin (Fig. 1) using the natural lasso peptide-producing strain

301 *Sphingomonas subterrenea* as a host [24].

302 The shuttle vector pHSG396Sp was constructed by integrating *par* region and *repA*

303 gene (shown in red, Fig. 2), following a previous report [8]. The promoter sequence of

304 TTGACA - 17bp - TANNNGC was reported as a high expression, efficiency promoter

305 sequence for *Sphingomonas* species [18, 19]. Thus, we integrated that promoter

306 sequence (TTGACA - 17bp - TAGAGGC) upstream of the brevunsin biosynthetic gene

307 cluster (*breA*, *breB*, and *breC*, shown in green, Fig 2), constructing the expression

308 vector pHSG396Sp-12697L (Fig. 2 and Fig. S2). The expression vector pHSG396Sp-

309 12697L was transformed into *S. subterrenea* using electroporation.

310 The bacterium *S. subterrenea*, harboring pHSG396Sp-12697L, was cultured using

311 modified basal medium (1 L) containing chloramphenicol. A new lasso peptide

312 brevunsin (10.2 mg) was isolated from the extract of the culture, along with the

313 previously reported lasso peptide subterisin [24]. As a control, *S. subterrenea* harboring

314 pHSG396Sp was also cultured and tested for production of brevunsin with same

315 condition. As a result, *S. subterrenea* harboring pHSG396Sp was confirmed to

316 produce subterisin but not brevunsin (Fig. S3). Brevunsin showed low solubility in

317 distilled water (less than 10 µg/mL) and high solubility (more than 1 mg/mL) in DMSO

318 and MeOH. To date, this yield (10.2 mg/L) is the highest yield for the heterologous
319 production of a lasso peptide, among previous reports [10-15, 40, 41]. The molecular
320 formula of brevunsin was confirmed to be C₉₉H₁₄₈N₂₄O₃₃S by accurate ESI-MS
321 analysis, because the ion corresponding to [M+2H]²⁺ was observed at *m/z* 1117.5244
322 (calculated *m/z* value: 1117.5253). The molecular formula was identical to what we
323 expected from the precursor gene sequence (Fig. 1). To obtain the chemical structure,
324 NMR experiments, including ¹H, ¹³C, DEPT-135, DQF-COSY, TOCSY, NOESY,
325 HMBC, and HSQC, were performed on brevunsin in 0.5 mL of DMSO-*d*₆. Assignment
326 of the constituent amino acids was accomplished using spin system identification (Table
327 S2), although several protons and carbons could not be determined, due to the broadness
328 of the signals in the NMR spectra. The three partial structures A-C were established
329 mainly by the analysis of the correlations from the TOCSY and NOESY experiments
330 (Fig. 3). To obtain further information about the amino acid sequence, MALDI-TOF
331 MS and MS/MS analyses was performed. The product ions for brevunsin from the
332 MALDI-TOF MS/MS analysis were suggested to correspond to the fragments of the *b*-
333 series (*b*₉-*b*₂₀) and *y*-series (*y*₃-*y*₅ and *y*₉-*y*₁₂), which indicated the sequence of Gly-
334 Leu-Val-Arg-Asp-Ser-Leu-Tyr-Pro-Pro-Ala-Gly at the C-terminus (Fig. 4a and Table
335 S3). To confirm the amino acid sequence of the macrolactam ring, a cleavage reaction at

336 the C-terminus peptide bond of Met was performed using cyanogen bromide (CNBr)
337 [6]. After the CNBr reaction, the cleaved brevunsin was purified by HPLC. The
338 molecular formula of the CNBr-cleaved brevunsin was confirmed to be $C_{98}H_{146}N_{24}O_{34}$
339 by accurate ESI-MS analysis, because the ion corresponding to $[M+H]^{2+}$ was observed
340 at m/z 1102.5282 (calculated m/z value: 1102.5289). In the CNBr reaction, the Met
341 residue of a peptide is reported to be transformed to homoserinelactone (HSL). The
342 MALDI-TOF MS/MS of the cleaved brevunsin gave the sequence of the branched
343 peptide with two new C-terminal ends (Fig 4b and Table S4). The product ions ($b'1$,
344 $b'2$, and $b'3$) indicated the sequence of Asp-Gly-HSL at one C-terminal end. In
345 addition, the product ions ($b5$, $b6$, $y12$, and $y13$) indicated Asp-Gly-HSL connected to
346 Glu. These data indicated that the α -amine group of the first Asp and the γ -carbonyl
347 group of the 8th Glu formed an isopeptide bond. The planer chemical structure of
348 brevunsin was determined as shown in Fig. 4a, in combination with the data from the
349 NMR analysis.

350 To determine the stereochemistries of the constituent amino acids in brevunsin, a
351 modified Marfey's method [7] was applied. Briefly, the hydrolysate of brevunsin was
352 derivatized with L-FDLA, and the stereochemistry of each amino acid was determined
353 using HPLC analysis, by comparison with standards (Fig. S21-34). As a result, all of the

354 constituent amino acids were determined to be in the L form. The three-dimensional
355 solution structure of brevunsin was calculated using the software program CNS, version
356 1.1, based on the distance and dihedral angle restraints determined from the NOE
357 intensities (Fig. S19) and $^3J_{\text{HN}\alpha}$ coupling constants (Fig 5). The macrolactam ring
358 consisted of nine amino acids, from Asp1 to Glu9 (yellow in Fig. 5b). The amino acids
359 Gly10, Leu11, Val12, and Arg13 formed a loop structure, and the C-terminal amino
360 acid residues Asp14 to Gly21 passed through the macrolactam ring. The structure of
361 brevunsin was a typical lasso structure, which indicated that the modified genes in the
362 brevunsin biosynthetic gene cluster functioned properly to generate the “lasso”
363 structure, even though brevunsin had an “unusual” N-terminal amino acid with Asp in
364 the core peptide sequence.

365 Thermostability test on brevunsin was performed following previous report [1]. If
366 unthreading of C-terminus linear peptide part in lasso structure happens during heating,
367 unthreaded peptide is detected normally with shorter retention time. In this experiment,
368 possible unthreaded brevunsin was not detected after heating treatment (95 °C for 1hr at
369 most), which indicated thermostability of brevunsin (Fig. S20). Macrolactam ring of
370 brevunsin comprises of nine amino acids, which is spatially larger than macrolactum
371 ring with seven or eight amino acids. Bulky amino acid Phe at 17th position could

372 contribute to the thermostability by functioning like “plug” not to unthread (Fig. S19).
373 Some lasso peptides have been reported to have antibacterial activities [35, 21, 17].
374 Therefore, we performed an antibacterial activity assay on brevunsin. Following a
375 previous report [22], the paper disk diffusion method was applied with testing
376 microorganisms (bacterial strains, including *Escherichia coli*, *Pseudomonas*
377 *aeruginosa*, *Bacillus subtilis*, *Staphylococcus aureus*, and *Micrococcus luteus*; yeast
378 strains, including *Saccharomyces cerevisiae*, *Schizosaccharomyces pombe*; and fungal
379 strains, including *Aspergillus niger* and *Aspergillus oryzae*. However, brevunsin did not
380 show any antibacterial activity at the dosage of 50 µg/disk.

381 In this report, we established a heterologous production system using *S. subterranea*
382 as a host and successfully produced a new lasso peptide, brevunsin. Many unexplored
383 lasso peptide gene clusters in proteobacteria remain to be explored for heterologous
384 expression [14]. To the best of our knowledge, this is the first report of the heterologous
385 production of a lasso peptide using bacteria that belong to *Sphingomonas* as a host. In
386 addition, the yield of the lasso peptide brevunsin (10.2 mg/L) was high enough to
387 perform structure determination using NMR and a biological activity test. We believe
388 that this heterologous production system is an efficient tool for the production of other
389 unexplored lasso peptides.

390

391 **References**

- 392 1. Allen CD, Chen MY, Trick AY, Le DT, Ferguson AL, Link AJ (2016) Thermal
393 Unthreading of the Lasso Peptides Astexin-2 and Astexin-3. ACS Chem Biol
394 11:3043-3051. doi:10.1021/acscchembio.6b00588
- 395 2. Brunger AT, Adams PD, Clore GM *et al.* (1998) Crystallography & NMR
396 system: a new software suite for macromolecular structure determination. Acta
397 Crystallogr D Biol Crystallogr 54:905-921
- 398 3. Budisa N (2013) Expanded genetic code for the engineering of ribosomally
399 synthesized and post-translationally modified peptide natural products (RiPPs).
400 Curr Opin Biotechnol 24:591-598. doi:10.1016/j.copbio.2013.02.026
- 401 4. Clore GM, Gronenborn AM, Nilges M, Ryan CA (1987) Three-dimensional
402 structure of potato carboxypeptidase inhibitor in solution. A study using nuclear
403 magnetic resonance, distance geometry, and restrained molecular dynamics.
404 Biochemistry 26:8012-8023
- 405 5. Clubb RT, Ferguson SB, Walsh CT, Wagner G (1994) Three-dimensional solution
406 structure of Escherichia coli periplasmic cyclophilin. Biochemistry 33:2761-
407 2772

- 408 6. Gross E, Witkop B (1962) Nonenzymatic cleavage of peptide bonds: the
409 methionine residues in bovine pancreatic ribonuclease. J Biol Chem 237:1856-
410 1860
- 411 7. Harada KI, Fujii K, Hayashi K, Suzuki M, Ikai Y, Oka H (1996) Application of
412 D,L-FDLA derivatization to determination of absolute configuration of
413 constituent amino acids in peptide by advanced Marfey's method. Tetrahedron
414 Lett 37:3001-3004. doi:[https://doi.org/10.1016/0040-4039\(96\)00484-4](https://doi.org/10.1016/0040-4039(96)00484-4)
- 415 8. Hayashi H, Kurusu Y (2014) Analysis of a DNA region from low-copy-number
416 plasmid pYAN-1 of *Sphingobium yanoikuyae* responsible for plasmid stability.
417 Biosci Biotechnol Biochem 78:510-515. doi:10.1080/09168451.2014.890029
- 418 9. Hayashi H, Kurusu Y (2014) DNA regions responsible for maintenance of
419 *Shingobium* plasmid pYAN-2. Microbes Environ 29:96-99
- 420 10. Hegemann JD, De Simone M, Zimmermann M *et al.* (2014) Rational
421 improvement of the affinity and selectivity of integrin binding of grafted lasso
422 peptides. J Med Chem 57:5829-5834. doi:10.1021/jm5004478
- 423 11. Hegemann JD, Fage CD, Zhu S, Harms K, Di Leva FS, Novellino E, Marinelli
424 L, Marahiel MA (2016) The ring residue proline 8 is crucial for the thermal
425 stability of the lasso peptide caulosegnin II. Mol Biosyst 12:1106-1109.

- 426 doi:10.1039/c6mb00081a
- 427 12. Hegemann JD, Zimmermann M, Xie X, Marahiel MA (2013) Caulosegnins I-
428 III: a highly diverse group of lasso peptides derived from a single biosynthetic
429 gene cluster. *J Am Chem Soc* 135:210-222. doi:10.1021/ja308173b
- 430 13. Hegemann JD, Zimmermann M, Xie X, Marahiel MA (2015) Lasso peptides: an
431 intriguing class of bacterial natural products. *Acc Chem Res* 48:1909-1919.
432 doi:10.1021/acs.accounts.5b00156
- 433 14. Hegemann JD, Zimmermann M, Zhu S, Klug D, Marahiel MA (2013) Lasso
434 peptides from proteobacteria: Genome mining employing heterologous
435 expression and mass spectrometry. *Biopolymers* 100:527-542.
436 doi:10.1002/bip.22326
- 437 15. Hegemann JD, Zimmermann M, Zhu S, Steuber H, Harms K, Xie X, Marahiel
438 MA (2014) Xanthomonins I-III: a new class of lasso peptides with a seven-
439 residue macrolactam ring. *Angew Chem Int Ed Engl* 53:2230-2234.
440 doi:10.1002/anie.201309267
- 441 16. Imbert M, Blondeau R (1999) Effect of light on germinating spores of
442 *Streptomyces viridosporus*. *FEMS Microbiol Lett* 181:159-163
- 443 17. Iwatsuki M, Tomoda H, Uchida R, Gouda H, Hirono S, Omura S (2006)

- 444 Lariatins, antimycobacterial peptides produced by *Rhodococcus* sp. K01-B0171,
445 have a lasso structure. *J Am Chem Soc* 128:7486-7491. doi:10.1021/ja056780z
- 446 18. Kaczmarczyk A, Vorholt JA, Francez-Charlot A (2013) Cumate-inducible gene
447 expression system for sphingomonads and other Alphaproteobacteria. *Appl*
448 *Environ Microbiol* 79:6795-6802. doi:10.1128/AEM.02296-13
- 449 19. Kaczmarczyk A, Vorholt JA, Francez-Charlot A (2014) Synthetic vanillate-
450 regulated promoter for graded gene expression in *Sphingomonas*. *Sci Rep*
451 4:6453. doi:10.1038/srep06453
- 452 20. Kersten RD, Yang YL, Xu Y, Cimermancic P, Nam SJ, Fenical W, Fischbach
453 MA, Moore BS, Dorrestein PC (2011) A mass spectrometry-guided genome
454 mining approach for natural product peptidogenomics. *Nat Chem Biol* 7:794-
455 802. doi:10.1038/nchembio.684
- 456 21. Knappe TA, Linne U, Zirah S, Rebuffat S, Xie X, Marahiel MA (2008) Isolation
457 and structural characterization of capistruin, a lasso peptide predicted from the
458 genome sequence of *Burkholderia thailandensis* E264. *J Am Chem Soc*
459 130:11446-11454. doi:10.1021/ja802966g
- 460 22. Kodani S, Inoue Y, Suzuki M, Dohra H, Suzuki T, Hemmi H, Ohnishi-
461 Kameyama M (2017) Sphaericin, a lasso peptide from the rare actinomycete

- 462 *Planomonospora sphaerica*. Eur J Org Chem:1177-1183.
463 doi:10.1002/ejoc.201601334
- 464 23. Koradi R, Billeter M, Wuthrich K (1996) MOLMOL: a program for display and
465 analysis of macromolecular structures. J Mol Graph 14:51-55, 29-32
- 466 24. Kuroha M, Hemmi H, Ohnishi-Kameyama M, Kodani S (2017) Isolation and
467 structure determination of a new lasso peptide subterisin from *Sphingomonas*
468 *subterranea*. Tetrahedron Lett 58:3429-3432.
469 doi:10.1016/J.TETLET.2017.07.064
- 470 25. Laskowski RA, Rullmann JA, MacArthur MW, Kaptein R, Thornton JM
471 (1996) AQUA and PROCHECK-NMR: programs for checking the quality of
472 protein structures solved by NMR. J Biomol NMR 8:477-486
- 473 26. Letzel AC, Pidot SJ, Hertweck C (2014) Genome mining for ribosomally
474 synthesized and post-translationally modified peptides (RiPPs) in anaerobic
475 bacteria. BMC Genomics 15:983. doi:10.1186/1471-2164-15-983
- 476 27. Li Y, Zirah S, Rebuffat S (2015) Lasso Peptides: Bacterial Strategies to Make
477 and Maintain Bioactive Entangled Scaffolds. Springer,
- 478 28. Link AJ (2015) Biosynthesis: Leading the way to RiPPs. Nat Chem Biol
479 11:551-552. doi:10.1038/nchembio.1862

- 480 29. Maksimov MO, Link AJ (2014) Prospecting genomes for lasso peptides. *J Ind*
481 *Microbiol Biotechnol* 41:333-344. doi:10.1007/s10295-013-1357-4
- 482 30. Maksimov MO, Pan SJ, James Link A (2012) Lasso peptides: structure,
483 function, biosynthesis, and engineering. *Nat Prod Rep* 29:996-1006.
484 doi:10.1039/c2np20070h
- 485 31. Maksimov MO, Pan SJ, James Link A (2012) Lasso peptides: structure,
486 function, biosynthesis, and engineering. *Nat Prod Rep* 29:996-1006.
487 doi:10.1039/c2np20070h
- 488 32. Maksimov MO, Pelczer I, Link AJ (2012) Precursor-centric genome-mining
489 approach for lasso peptide discovery. *Proc Natl Acad Sci U S A* 109:15223-
490 15228. doi:10.1073/pnas.1208978109
- 491 33. Martin-Gomez H, Tulla-Puche J (2018) Lasso peptides: chemical approaches
492 and structural elucidation. *Org Biomol Chem*. doi:10.1039/c8ob01304g
- 493 34. Metelev M, Tietz JI, Melby JO, Blair PM, Zhu L, Livnat I, Severinov K,
494 Mitchell DA (2015) Structure, bioactivity, and resistance mechanism of
495 streptomomicin, an unusual lasso Peptide from an understudied halophilic
496 actinomycete. *Chem Biol* 22:241-250. doi:10.1016/j.chembiol.2014.11.017
- 497 35. Salomon RA, Farias RN (1992) Microcin 25, a novel antimicrobial peptide

- 498 produced by *Escherichia coli*. J Bacteriol 174:7428-7435
- 499 36. Sardar D, Schmidt EW (2016) Combinatorial biosynthesis of RiPPs: docking
500 with marine life. Curr Opin Chem Biol 31:15-21.
501 doi:10.1016/j.cbpa.2015.11.016
- 502 37. Solbiati JO, Ciaccio M, Farias RN, Salomon RA (1996) Genetic analysis of
503 plasmid determinants for microcin J25 production and immunity. J Bacteriol
504 178:3661-3663
- 505 38. Tietz JI, Schwalen CJ, Patel PS, Maxson T, Blair PM, Tai HC, Zakai UI,
506 Mitchell DA (2017) A new genome-mining tool redefines the lasso peptide
507 biosynthetic landscape. Nat Chem Biol. doi:10.1038/nchembio.2319
- 508 39. Wuthrich K, Billeter M, Braun W (1983) Pseudo-structures for the 20 common
509 amino acids for use in studies of protein conformations by measurements of
510 intramolecular proton-proton distance constraints with nuclear magnetic
511 resonance. J Mol Biol 169:949-961
- 512 40. Zimmermann M, Hegemann JD, Xie X, Marahiel MA (2013) The astexin-1
513 lasso peptides: biosynthesis, stability, and structural studies. Chem Biol 20:558-
514 569. doi:10.1016/j.chembiol.2013.03.013
- 515 41. Zong C, Wu MJ, Qin JZ, Link AJ (2017) Lasso peptide benenodin-1 is a

516 thermally actuated [1] rotaxane switch. J Am Chem Soc 139:10403-10409.

517 doi:10.1021/jacs.7b04830

518

519 **Acknowledgments**

520 This study was supported by the Japan Society for the Promotion of Science by Grants-

521 in-aids (grant number 16K01913). We thank Ms. Tomoko Sato for measurement of

522 MS/MS data.

523 **Additional information**

524 Supplementary information accompanies this paper online.

525 **Competing Interests:** The authors declare that they have no competing interests.

526

527 Figure legends

528

529 Figure 1. Biosynthetic gene cluster of brevunsin

530 Figure 2. Construction of heterologous expression vector pHSG396Sp-12697L,

531 underlined letter indicates promoter sequence, bold letter indicates XbaI recognition site

532 Figure 3. Key 2D NMR correlations to construct three partial structures A-C (bold line:

533 TOCSY, double ended arrow: NOESY)

534 Figure 4. a) MS/MS experiment on brevunsin, b) MS/MS experiment on CNBr-cleaved

535 brevunsin

536 Figure 5. NMR-derived structures of brevunsin: (a) superposition of the 15 lowest-

537 energy structures and (b) the lowest-energy structure of brevunsin. The isopeptide bond

538 between Asp1 and Glu9 is shown in red. The ring-forming residues are shown in

539 yellow, and the loop and the tail in blue.

540

541 Figure legends

542

543 Figure 1. Biosynthetic gene cluster of brevunsin

544 Figure 2. Construction of heterologous expression vector pHSG396Sp-12697L,

545 underlined letter indicates promoter sequence, bold letter indicates XbaI recognition

546 site.

547 Figure 3. Key 2D NMR correlations to construct three partial structures A-C

548 Figure 4. a) MS/MS experiment on brevunsin, b) MS/MS experiment on CNBr-cleaved

549 brevunsin

550 Figure 5. NMR-derived structures of brevunsin: (a) superposition of the 15 lowest-

551 energy structures and (b) the lowest-energy structure of brevunsin. The isopeptide bond

552 between Asp1 and Glu9 is shown in red. The ring-forming residues are shown in

553 yellow, and the loop and the tail in blue.

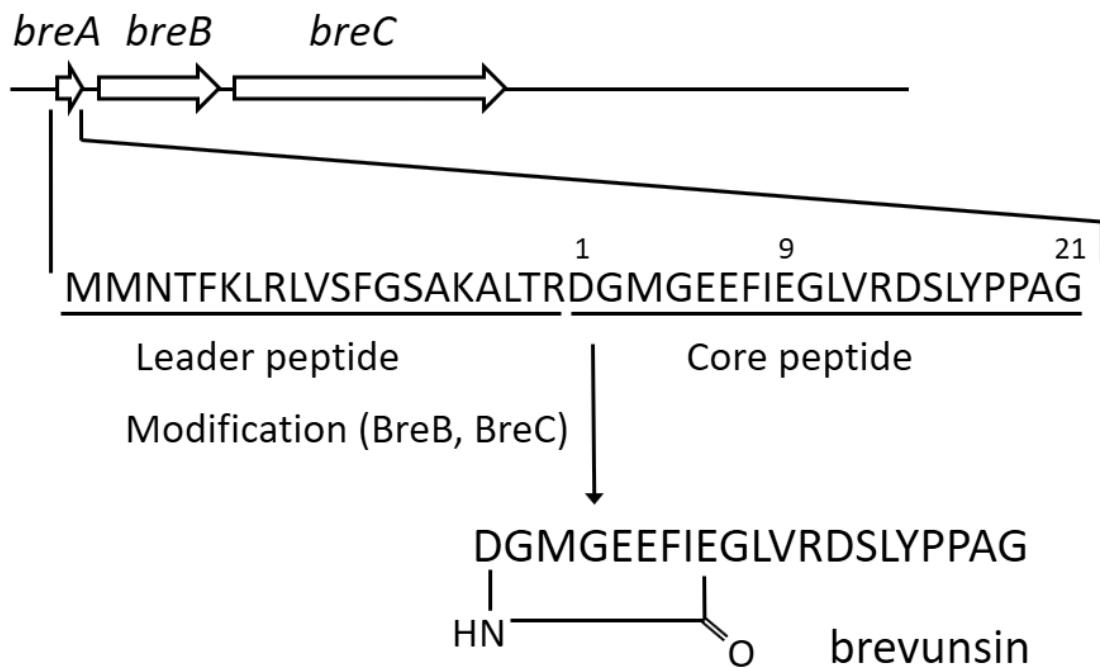
554

555 Figure 1

556

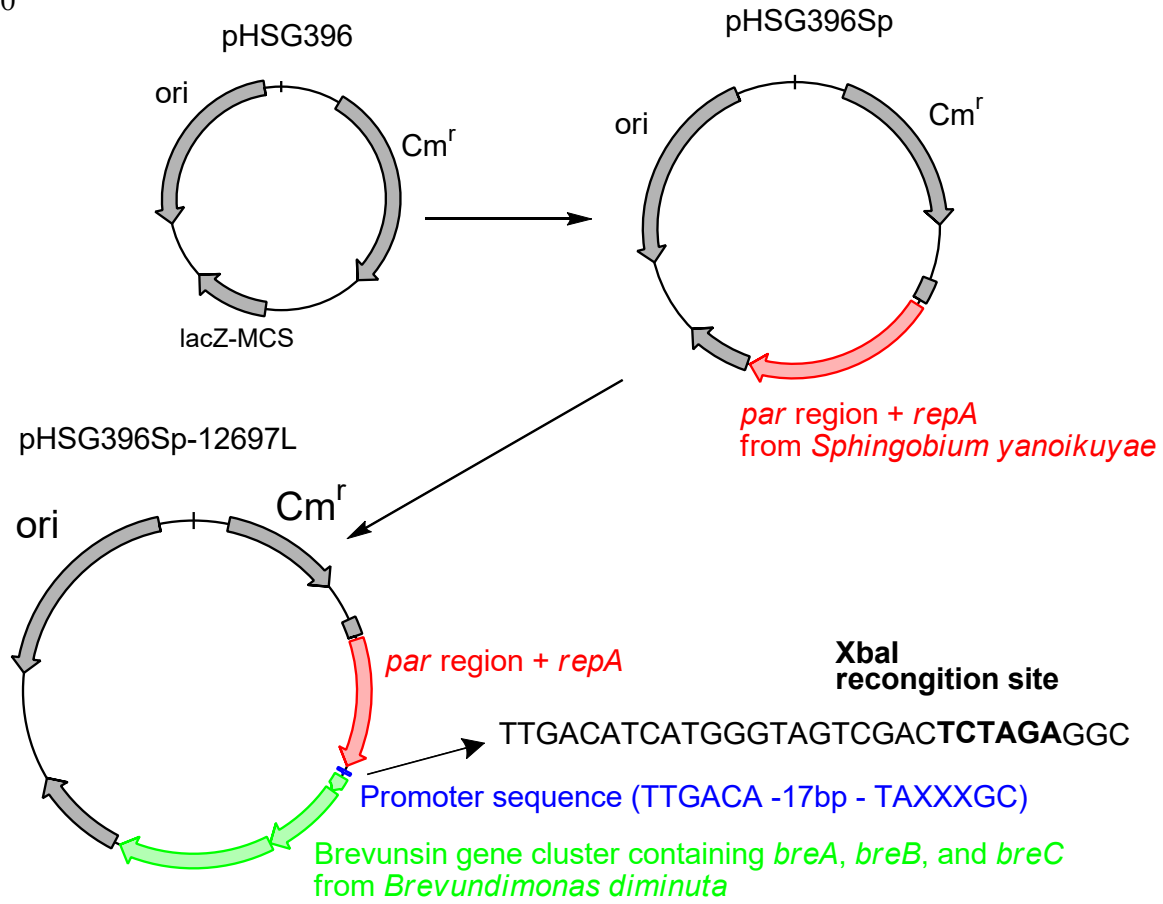
557

558

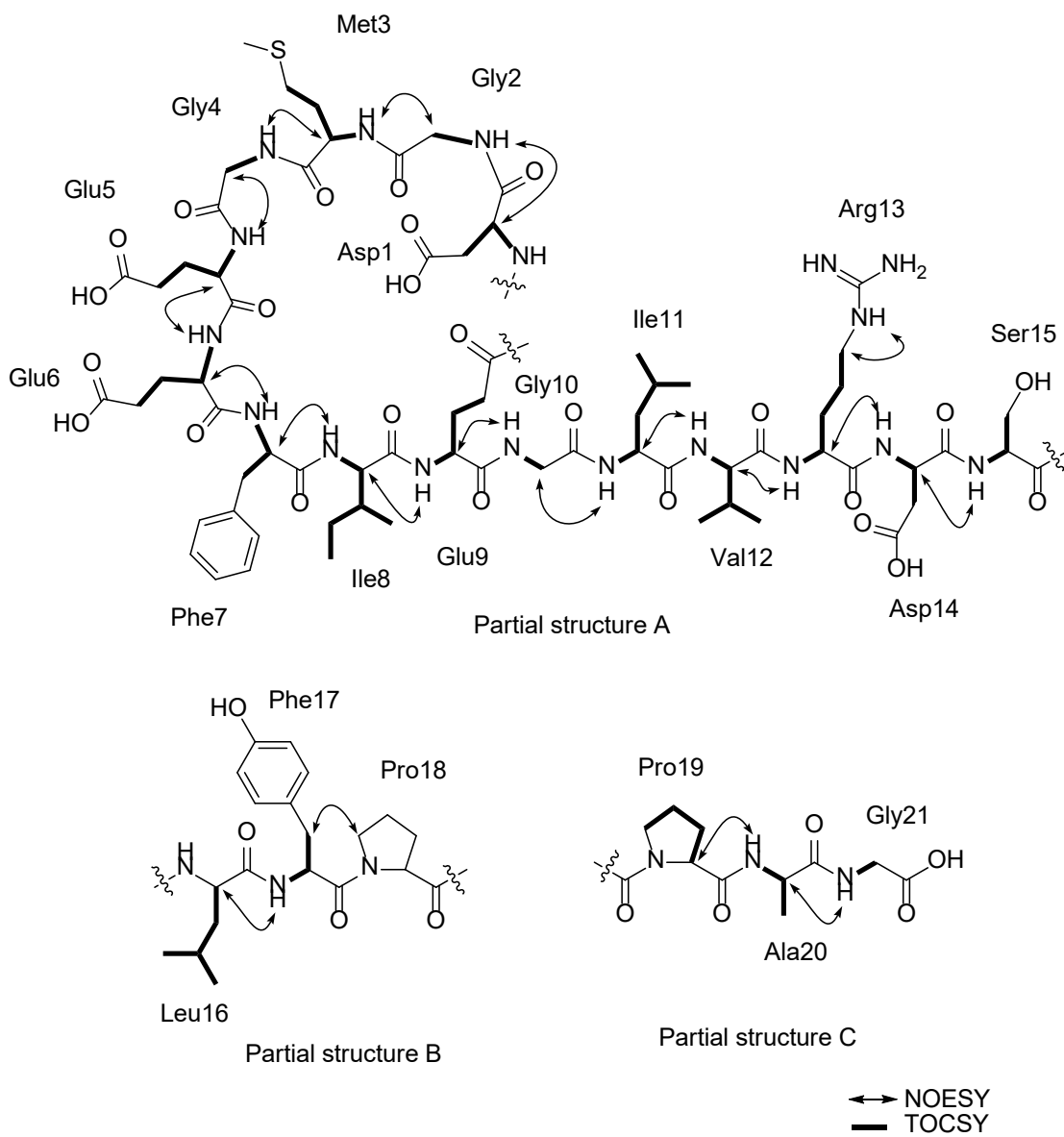


559 Figure 2

560

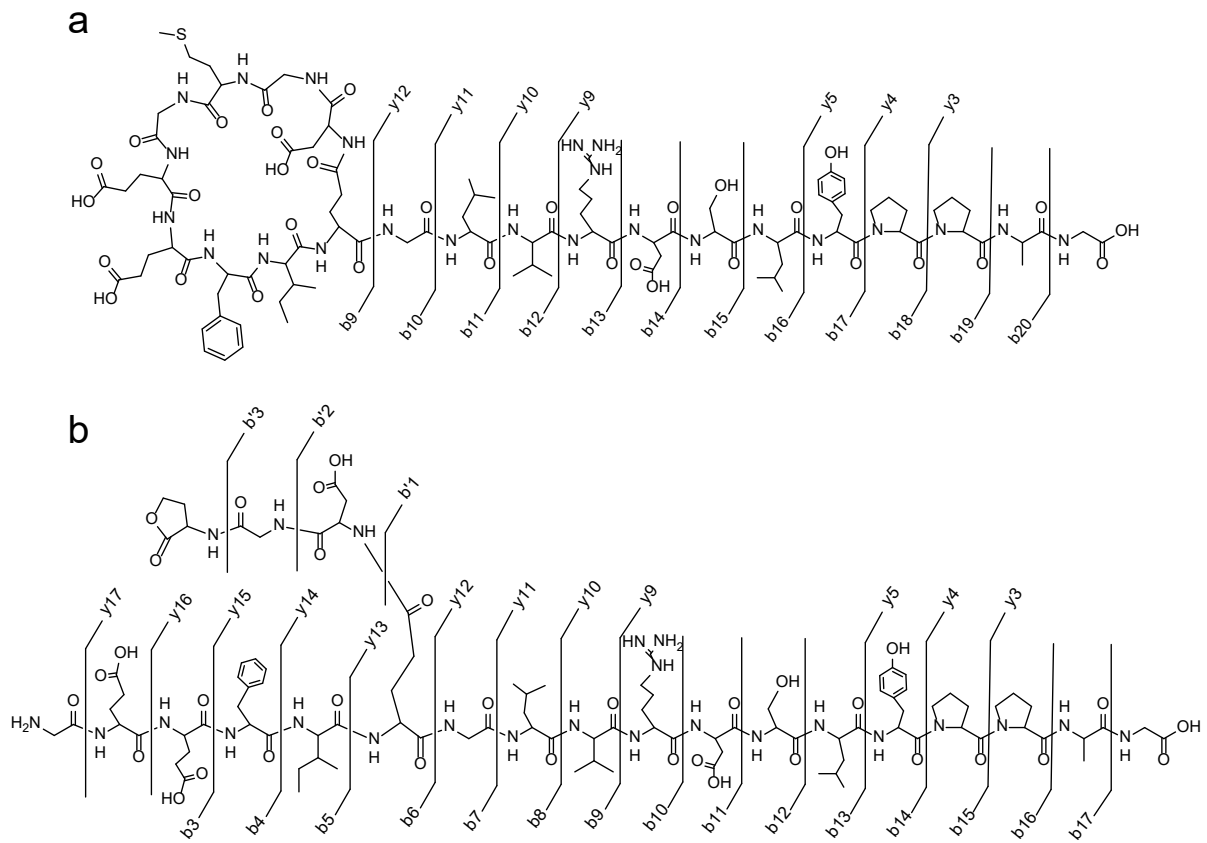


561 Figure 3



562 Figure 4

563



564 Figure 5

565

566

